WPPMI-PR(17) 18122

RP Wenninger et al.

Progress in the physics understanding for a conceptual design of DEMO

Preprint of Paper to be submitted for publication in
Plasma Physics and Controlled Fusion

This work has been carried out within the framework of the EUROfusion Consortium and has received funding from the Euratom research and training programme 2014-2018 under grant agreement No 633053. The views and opinions expressed herein do not necessarily reflect those of the European Commission.

Progress in the physics understanding for a conceptual design of DEMO

R. Wenninger[1,2], C. Bachmann[1], M. Beckers[3], M. Cavedon[2], D. Coster[2], M. Dunne[2], T. Eich[2], E. Fable[2], A. Fasoli[4], G. Federici[1], T. Görler[2], J. Graves[4], T.C. Hender[1], Y.Q. Liu[5,6], F. Maviglia[1], G. Maddaluno[7], T. Pütterich[2], H. Reimerdes[4], S. Saarelma[8], M. Siccinio[2], B. Sieglin[2], F. Subba[9], F. Villone[10], J.H. You[2], L.N. Zhou[11], H. Zohm[2]

[1]EUROfusion Programme Management Unit, Garching, Germany
[2]Max-Planck-Institut für Plasmaphysik, Garching, Germany
[3]Institute of Energy- and Climate Research, Forschungszentrum Jülich GmbH; Germany
[4]École Polytechnique Fédérale de Lausanne, Swiss Plasma Center, CH-1015 Lausanne, Switzerland
[5]General Atomics, PO Box 85608, San Diego, CA 92186-5608, USA
[6]Southwestern Institute of Physics, PO Box 432, Chengdu 610041, China
[7]ENEA Frascati, C.P. 65, 00044 Frascati, Rome, Italy
[8]Culham Centre for Fusion Energy, Culham Science Centre, Abingdon, UK
[9]NEMO group, dipartimento di Energetica, Politecnico, I-10129 Torino, Italy
[10]Università di Cassino, Italy
[11]Key Laboratory of Materials Modification by Laser, Ion, and Electron Beams (Ministry of Education), School of Physics and Optoelectronic Technology, Dalian University of Technology, Dalian 116024, China

E-mail: ronald.wenninger@euro-fusion.org

Abstract. In the European fusion roadmap ITER is followed by a demonstration fusion power plant (DEMO), with the capability of generating several hundred MW of net electricity and operating with a closed fuel-cycle. The ongoing development of a conceptual design for DEMO implies predominantly engineering efforts. However, as input for these activities and for the identification of the optimum set of overall design parameters for DEMO, also a variety of open physics questions related to the feasibility or the performance of investigated DEMO designs must be answered.
This paper provides an overview of essential DEMO Physics Gaps and illustrate some consequences on the DEMO design development. Furthermore several areas, in which the DEMO Physics Basis has been significantly developed in recent years will be discussed:
ELMs: An initial concept for ex-vessel Resonant Magnetic Perturbation (RMP) coils (n=1-3), which according to most recently developed criteria effectively mitigate ELMs in DEMO, is presented. Also, potential performance reductions associated with ELM mitigation/suppression schemes are discussed.
Divertor protection: An overview of 0D power exhaust parameters for a recent DEMO design is presented. Also, largely consistent parameters of a reduced SOLPS simulation for DEMO are presented.
First wall loads: A brief overview of the status of the investigation of loads on the first wall of DEMO is provided. There is indication, that the non-disruptive part of these loads can be handled by appropriate design choices. However, these solutions might be associated with reduced gross electric power or T breeding ratio.
Disruptions: Investigation of the heat impact during unmitigated disruptions

show heat impact factors clearly above the melt threshold during vertical displacement events (first wall) and central disruptions (divertor). Several aspects of a disruption strategy for DEMO are discussed.

1. Introduction

The European fusion raodmap [1] defines the development of a conceptual design for a demonstration fusion power plant (DEMO) as one of the main priorities of the recent European fusion program. This activity implies extensive engineering efforts dedicated to the conceptual design of individual machine components (e.g. breeding blanket or divertor) and the design integration of these components. In addition there is a lot of information on the physics in DEMO to be provided. A part of this information is important for the assessment of the feasibility or the overall performance of the plant and hence it is crucial for the DEMO Design Point Development [2]. Another part is important input to the development of concepts of individual components. For instance information on plasma wall loads [3] have to be provided to the wall designers. DEMO has significantly different requirements than ITER and consequently significantly different plasma conditions [4]. Consequently there are gaps in our physics knowledge, which do not necessarily need to be closed to operate ITER, but which need to be closed for the DEMO design development or operation. We refer to all of these gaps as *DEMO Physics Gaps*, irrespective of the question, when in the evolution of DEMO the knowledge will be required. An overview of DEMO Physics Gaps, as it is introduced in section 2, is of central importance for the prioritization of DEMO physics activities and the identification of potential show-stoppers.
In Europe a systematic program to develop the *DEMO Physics Basis* and to close at the same time DEMO Physics Gaps has been launched in 2014. Although investigations in many areas are ongoing, there is a number of interesting results. While a first set of these results has already been published [4], in this paper various new findings are presented in section 3.
The investigations presented in this paper are based on the design `EU DEMO1 2015` [2].

2. DEMO Physics Gaps

DEMO will be significantly different to ITER in terms of design and mission [5]. Consequently, there are gaps in our physics knowledge, which do not need to be closed to operate ITER, but which need to be closed (1) to complete the conceptual design for, or (2) to complete the engineering design for DEMO, or (3) to operate DEMO.
Certainly, the boundaries are not in any case perfectly sharp. There are several areas, in which the knowledge is interesting for ITER, but essential for DEMO. Also, in some areas the problems have to be addressed separately for DEMO and ITER due to the different machine and plasma design. In the following we provide a list of key DEMO Physics Gaps. We differentiate between gaps that are required to be closed to ensure the feasibility of DEMO designs and gaps that are required to be closed to predict the plasma performance correctly. However, performance gaps imply significant uncertainties with respect to the ratio of net electric power output and capital cost. For instance, it has been shown that the extensive uncertainty on the

LH-threshold power translates into a similar relative uncertainty of the major radius [2]. Hence, a significant reduction of these gaps is required before the finalization of the design of DEMO.
In this publication we can only present the most urgent questions with a low level of detail. These questions can be broken down in more detailed question, which need to be answered by experiments and/or by theory and modelling.
Feasibility gaps:

- *Disruptions*: (See also subsection 3.4.) A DEMO concept needs to include evidence of safety and machine protection. To provide this (1) the characteristics and damaging effect of worst case disruptions need to be predicted and (2) the rates of these events need to be estimated for a fully disruptivity-optimised DEMO. There are significant gaps associated with the extrapolation of thermal loads and runaway electron loads for mitigated and un-mitigated disruptions in DEMO. Also, their is currently almost no basis for the prediction of rates of disruptions in DEMO and real-time control algorithms to avoid and recover from disruptive situations need to be developed.
- *Tolerable ELMs*: (See also subsection 3.1.) It has been understood that the natural occurring type I edge localized modes (ELMs) in DEMO are not tolerable due to excess of the divertor surface temperature limit [6]. Hence it is of key importance to demonstrate an ELM mitigation method or a no/small ELM regime, which reduces the ELM loads to an acceptable level. For all identified candidate scenarios/methods significant gaps concerning the extrapolabillity of the scenario to DEMO or the effectiveness of the load reduction in DEMO have to be closed.
- *Protection of an ITER-like divertor*: (See also subsection 3.2.) Compared to ITER the total heating power in recent European DEMO designs is ≈ 4, while the major radius is ≈ 1.5 times higher. Due to this the strategy is to have a higher amount of core radiation from seeded impurities. However, this is only possible as long the power crossing the pedestal region is sufficient to operate robustly in H-mode. Hence also the divertor might have to process a higher power density than in ITER. Initial simulations of the pedestal, SOL and divertor plasma in DEMO with a reduced version of SOLPS suggest that this is possible as long as the electron density at the separatrix $n_{e,sep}$ is high enough (subsection 3.2). The predictive capability of these codes including the prediction of the transport coefficients needs to be significantly consolidated. Also the question on the consistency of the required $n_{e,sep}$ with the pedestal and core needs to be clarified.
- *Alternative exhaust strategies*: For the case that the protection of an ITER-like divertor cannot be achieved in DEMO, a significant program of investigating alternative exhaust strategies is ongoing in Europe [7]. For the case of a magnetic double-null configuration [8] such modifications can have impact on many other aspects (e.g. L-H-power threshold or pedestal top height). Often the physics basis in these areas is much weaker than for an ITER-like configuration and hence many related gaps have to be closed.
- *Impurity transport*: The transport of impurities (He, W and seed impurities like Ar) in the core and pedestal of DEMO is subject to considerable uncertainties. This is also due to uncertainties in the background profiles and ELM situation.

At the upper end of the resulting impurity concentration range the burn condition is not fulfilled anymore [9].

- *Momentum transport*: The rotation profile has effects on the global stability and neoclassical tearing mode. It is important to achieve predictability of the rotation profile and these effects for DEMO.
- *Fast particles*: The interaction of fast particles and Alfvenic modes can cause a significant modification on the radial distribution of fast particles and thermal particles. If these effects are extreme, fast particle losses or a reduction of confinement can be significant [10]. These effects have to be studied for DEMO including their relation to the burn dynamics.

Performance gaps:

- *Core heat and particle transport*: Gyrokinetic ab initio simulations show good agreement to measurements for many experimental scenarios. However, in view of DEMO, a few gaps still needs to be filled (e.g. related to electromagnetic and fast ion stabilization effects).
- *Pedestal transport* : For the prediction of the pedestal pressure shape, the code EPED [11] is frequently applied. However it is unclear, if the code for DEMO has the same prediction quality as for present devices. Aspects like SOL condition, radiation fraction and edge perturbations (e.g. ELMs) might be quite different. Also, the prediction of the pedestal top density needs to improve significantly.
- *L-H power threshold*: The ITPA scaling of the L-H-threshold power $P_{LH,thr}$ applied to ITER has an upper limit of the 95% confidence interval that corresponds to twice the scaled value [12]. As this scaling has been developed for ITER, it is expected that the uncertainty is more extreme for DEMO. At fixed divertor performance expressed in P_{sep}/R and peak field at the TF coil conductor, this uncertainty of $P_{LH,thr}$ corresponds to an uncertainty of ≈ 2 in terms of major radius, if net electric power output and pulse duration are fixed.
- *Blob activity*: There are several open questions about how the blob activity in the SOL extrapolates to DEMO [13]. In the most extreme case a significant amount of power crossing the separatrix could be distributed radially with an e-folding length of up to 50mm at the outer mid-plane. This would lead to the necessity of relatively large gaps and and lower elongation and hence reduces the performance [2].

3. Progress in the DEMO Physics Basis Development

3.1. Edge Localized Modes

Edge Localized Modes (ELMs) [14] can play an important role in flushing impurities out of the pedestal plasma. On the other side they can lead to significant divertor erosion and high local energy impact factors at the first wall via filaments and the divertor. For a first assessment the ITER limit for the ELM energy density $\varepsilon_{div} = 0.5MJ/m^2$, which corresponds to the W surface melt limit, can be applied. An initial prediction of the divertor loads for natural type I ELMs in `EU DEMO1 2015` came to the conclusion that the relative energy loss per ELM $\Delta W_{th}/W_{th}$ has to be reduced by a factor 15 to 90 [6]. Here the ELM energy density has been estimated based on ΔW_{th}, the inter-ELM wetted area and a range of assumptions on the broadening of the divertor

footprint during ELMs.
This underlines the need to find an ELM mitigation method that is compatible with acceptable loads and erosion rates. An initial review identified candidates including operational regimes with small or no ELMs (e.g. QH-mode[15], type II ELMs[16], I-mode[17]) and the application of appropriate actuators (e.g. RMP ELM mitigation/suppression[18, 19]). For all of these candidates substantial R&D has to be carried out to assess the feasibility of the associated concept in DEMO.

3.1.1. RMP ELM mitigation The possibility of RMP ELM mitigation in DEMO has been investigated. The MARS-F code [20] has been used to compute the linear plasma response to the 3D magnetic field perturbations generated by the ELM control coils. This computed plasma response allows to establish certain figures of merit, that are then used to guide the ELM control coil design for DEMO.
The investigations reported here are based on two toroidal rows of window frame coils. The rows are on the outboard side between upper and mid-plane port respectively between mid-plane port and divertor port as illustrated in figure 1 (a). Along the toroidal angle, it is assumed that there is a sufficient number of coils, to produce the desired toroidal mode number n. Two possible radial locations of the coils are considered: just outside the inner vacuum vessel (OIVV), or just outside the outer vacuum vessel (OOVV). The possibility of the technical integration of the coils into DEMO is assessed as *unclear* for OIVV and *feasible* for OOVV. The poloidal location of each row of coils is specified by the poloidal angle θ_c of the center of each coil. The size of each coil, along the poloidal angle, is specified by the poloidal coverage angle $\Delta\theta$.

The figures of merit, that is used to optimize the coil design, is related to the so called edge-peeling response from the plasma induced by the applied vacuum RMP field. The edge-peeling response yields a large plasma surface displacement near the x-point ξ_x. An example is shown in figure 1 (b). Extensive comparison between modeling and present day ELM control experiments reveals that a large x-point displacement is always associated with favorable ELM control, either mitigation or suppression [21, 22, 23, 24, 25, 26, 27].
It is possible to establish a semi-empirical criterion for ELM mitigation, by computing the MHD model predicted x-point displacement for experimental plasmas exceeding the current threshold for ELM mitigation. Following critical x-point displacements $\xi_{x,c}$ have been observed: ASDEX Upgrade: $\xi_{x,c} = 1.5mm$ ($n = 2$), MAST: $\xi_{x,c} = 1.5mm$ ($n = 4$ and 6) [28, 29], JET: $\xi_{x,c} = 2.8mm$ ($n = 2$), DIII-D: $\xi_{x,c} = 0.9mm$ ($n = 3$, ELM suppression). Hence, $\xi_{x,c} = 10mm$ is a conservative target value for DEMO.
For $n = 1 - 6$ it is found that the closer the RMP coils are located to the plasma, the less coil current is required in order to obtain the same level of ξ_x. The optimal coil phasing depends nearly linearly on θ_c and is less sensitive to $\Delta\theta$. At fixed poloidal location of the coils, the optimal coil size tends to decrease with increasing n. However, for $n = 3 - 6$, the optimal coil size is found to be $\Delta\theta \approx 40°$. For a fixed coil geometry, the computed x-point displacement strongly depends on the choice of the coil phasing $\Delta\Phi$.

Figure 2 shows a typical examples for n=3 and a coil current amplitude of 200 kAt. For a chosen coil geometry, ξ_x is sensitive to the coil phasing. Though interestingly, the optimal phasing is not sensitive to the coil size. Figure 3 shows the computed ξ_x versus the ELM control coil current amplitude for OOVV configurations at optimized

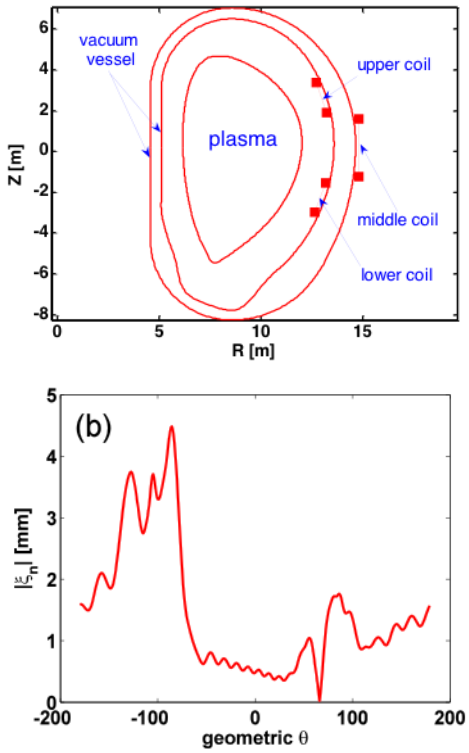

Figure 1. (a) The plasma boundary shape and the inner and outer vacuum vessel contour for DEMO. The locations of the ELM control coils are only indicative. (b) An example of the MARS-F computed plasma surface displacement along the poloidal angle (in degrees). The x-point is located near $\theta = -100°$.

$\Delta\Phi$. For $n \leq 3$ the criterion $\xi_{x,c} \leq 10mm$ can be satisfied for $I_C < 200kAt$. There might be even some optimization potential in terms of θ_c and $\Delta\theta$.

In summary this investigation provides evidence that ELM mitigation in DEMO with ex-vessel coils is feasible. However, ELM mitigation is usually understood as a significant reduction of the ELM energy loss and the effect on the divertor is not uniquely defined. Hence, it is not clear, if ELM mitigation in DEMO is sufficiently reducing the ELM divertor energy density. This could be resolved by the development of a criterion for RMP ELM suppression that can be applied to DEMO.

3.1.2. Effect of ELM mitigation on the pedestal It is very likely that the reduction of the ELM energy density at the divertor by any mitigation method leads to a performance reduction in DEMO due to a degradation of the pedestal. Recently a scaling of the parallel ELM energy density $\varepsilon_{\parallel}$ with the pedestal top density $n_{e,ped}$, the pedestal top temperature $T_{e,ped}$ and the relative ELM size ΔE_{ELM} based on data from JET, AUG and MAST has been presented [30]. So far there is no evidence that any mitigation method has the potential to diverge significantly from this scaling. Applying the scaling to DEMO with $n_{e,ped,0} = 0.67 \times 10^{20} m^{-3}$, $T_{e,ped,0} = 5.5keV$, $\Delta E_{ELM,0} = 10\%$ and a target inclination $\alpha = 3°$ leads to $\varepsilon_{div} = 1.8MJ/m^2$. This corresponds to $5.4MJ/m^2$ obtained by the approach presented in [6]. Table 1 shows

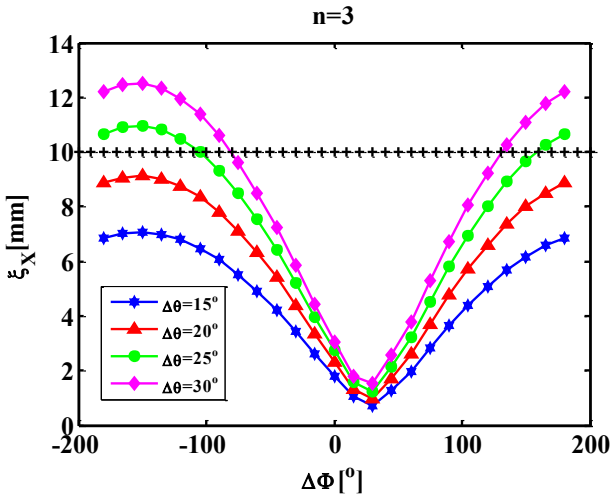

Figure 2. x-point plasma displacement computed by MARS-F as a function of $\Delta\Phi$, for n=3 and for various $\Delta\theta$. Considered are the upper and lower rows of coils located outside the outer VV, at the poloidal angle of $\mid \theta_c \mid = 30°$. The coil current amplitude is assumed to be 200 kAt. The horizontal line indicates the $\xi_x = 10mm$ displacement level.

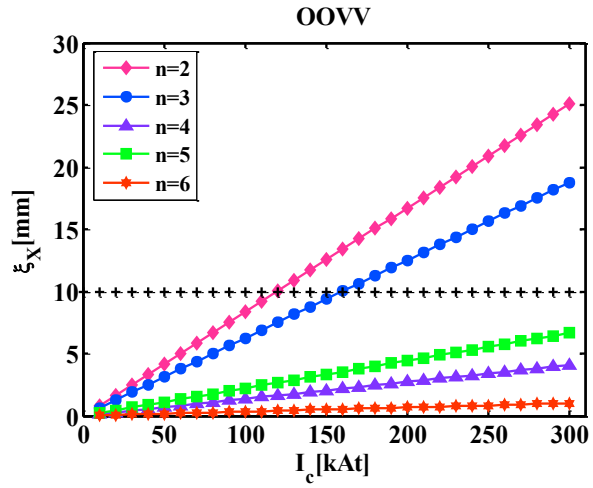

Figure 3. x-point plasma displacement as a function of the coil current I_C computed by MARS-F versus the ELM control coil current amplitude, for different choices of the toroidal mode number n=2-6 for OOVV. Considered are upper and lower rows of coils, with the coils poloidal size and location being chosen as $\mid \theta_c \mid = 30°$, $\theta_c = 30°$. The toroidal coil phasing between the upper and lower rows of the coil current is already optimized. The horizontal line indicates the $\xi_x = 10mm$ displacement level.

possible combinations of reduced pedestal parameters to achieve $\varepsilon_{div} = 0.5MJ/m^2$. Table 2 displays the same values relative to $n_{e,ped,0}$, $T_{e,ped,0}$ and $\Delta E_{ELM,0}$. If only one parameter is changed, it needs $n_{e,ped} = 0.18 \times n_{e,ped,0}$ or $T_{e,ped} = 0.27 \times T_{e,ped,0}$ or $\Delta E_{ELM} = 0.08 \times \Delta E_{ELM,0}$. More easy to achieve could be a combination like

Table 1. Possible combinations of reduced pedestal parameters to achieve $\varepsilon_{div} = 0.5MJ/m^2$: $\Delta E_{ELM}[\%]$ as a function of $n_{e,ped}$ and $T_{e,ped}$.

		$n_{e,ped}[10^{20}m^{-3}]$					
		0.67	0.56	0.45	0.34	0.23	0.12
$T_{e,ped}$ $[keV]$	5.5	1.1	1.4	2.0	3.0	5.3	13.5
	4.7	1.6	2.0	2.8	4.3	7.5	19.4
	3.9	2.4	3.2	4.4	6.6	11.8	30.2
	3.1	4.4	5.7	7.8	11.8	20.9	53.9
	2.3	10.0	13.0	18.0	27.1	48	123.5

Table 2. Possible combinations of reduced pedestal parameters to achieve $\varepsilon_{div} = 0.5MJ/m^2$: $\Delta E_{ELM}/\Delta E_{ELM,0}$ as a function of $n_{e,ped}/n_{e,ped,0}$ and $T_{e,ped}/T_{e,ped,0}$.

		$n_{e,ped}/n_{e,ped,0}$					
		1	0.8	0.7	0.5	0.3	0.2
$T_{e,ped}/T_{e,ped,0}$	1	0.1	0.1	0.1	0.2	0.4	1.0
	0.9	0.1	0.1	0.2	0.3	0.5	1.4
	0.7	0.2	0.2	0.3	0.4	0.8	1.9
	0.6	0.2	0.3	0.4	0.7	1.2	3.0
	0.4	0.4	0.6	0.8	1.2	2.1	5.4

$n_{e,ped} = 0.7 \times n_{e,ped,0}$, $T_{e,ped} = 0.7 \times T_{e,ped,0}$ and $\Delta E_{ELM} = 0.3 \times \Delta E_{ELM,0}$. Assuming a reduction of $\Delta E_{ELM} = 10\%$ is not possible, a simultaneous reduction of pedestal top density and temperature to 48% of the values above would correspond to $\varepsilon_{div} = 0.5MJ/m^2$.

3.2. Steady state divertor protection

Handling the exhaust of power and particles in DEMO has been identified as one of the central challenges [1]. The design `EU DEMO1 2015` includes a lower single-null magnetic configuration in combination with an ITER-like divertor in closed configuration and W mono-blocks. In Europe, also alternative divertor design options [7] and especially a double-null magnetic configuration [31] are investigated in terms of physics and engineering. The main power exhaust strategy for DEMO is to significantly increase the level of impurity seeding into the pedestal, SOL and divertor regions to have a higher total radiated power, which is distributed more homogeneously compared to power that is conducted or convected.

3.2.1. Divertor technology development The European fusion program includes a substantial project on divertor solutions with the primary objectives to devise advanced design solutions (starting from ITER-like technology) and to develop related technologies tailored for the DEMO-relevant operational environment [32]. The major difference in loading conditions of divertor plasma-facing components (PFCs) between DEMO and ITER are neutron irradiation damage of materials (ITER: 0.5dpa, DEMO: 13dpa for CU and 3 dpa for W), pulse duration (ITER: $\approx 440s$, DEMO: $\approx 7200s$) and coolant temperature (ITER: $100°C$, DEMO: $130°C$) [33, 34]. The higher irradiation dose in DEMO raises critical material issues for design, in particular, low-temperature embrittlement due to lattice damage and transmutation. The higher

coolant temperature is favored to mitigate irradiation embrittlement but is likely to locally overheat the structural material (heat sink) of the PFCs. Thus long-term strength at elevated temperature is required for the heat sink together with high toughness at lower temperature [35].
As baseline PFC design, a water-cooled tungsten monoblock model is considered, which is based on the ITER divertor PFC consisting of tungsten armor blocks surrounding a CuCrZr alloy cooling pipe joined with a thick copper interlayer [34, 36]. Although this model has survived many high-heat-flux fatigue tests under the loading conditions of ITER specifications [37], it is still not assured if the baseline PFC design is compatible with the DEMO operation conditions [38]. In an effort to address these issues and to propose solutions for the engineering challenges, 8 different novel design concepts are being developed where advanced materials [39] (W wire-reinforced Cu composite tube, W/Cu composite block, W/Cu laminate interlayer, chromium block, etc.) or nonconventional design approaches [34] (compositionally graded thin interlayer, thermal break layer, castellation, etc.) are employed.
In the last two years a significant progress has been achieved with regard to PFC design as well as technology development. Small scale mock-ups were fabricated by means of dedicated joining processes and nondestructive inspection techniques. The mock-ups were tested in a hydrogen beam irradiation facility (GLADIS) to evaluate high-heat-flux fatigue performance using cold as well as hot ($130°C$) coolant water. The mock-ups of 4 design concepts have withstood up to now at least 100-300 loading cycles at $20MW/m^2$ (screening test: 5 cycles up to $25MW/m^2$) while the testing of the other concepts are still ongoing. In addition, the pipework of the PFC cooling circuit for the vertical targets has been designed. Full 3D computational fluid dynamics analysis verified that the optimized cooling system delivered a sufficient power exhaust capability required for the target PFCs (106MW in total) with a reasonable thermo-hydraulic performance [40, 41].
The major impacts of fast neutron irradiation on the thermal and structural performance of the DEMO divertor targets are (1) reduced fatigue lifetime due to the embrittlement of the Cu interlayer, (2) increased risk of global fracture of W armour blocks due to embrittlement and (3) loss of high-temperature strength of the CuCrZr pipe due to irradiation creep [42, 43]. The underlying design rationales to mitigate or to overcome such detrimental effects are

- to employ a Cu-base composite material(s) which is immune to radiation-enhanced softening (irradiation creep) of CuCrZr alloy,
- to replace the thick Cu interlayer with a very thin bond coating for avoiding the pronounced embrittlement feature of pure Cu caused by radiation-induced transmutation,
- to reduce the dimension of W monoblocks or to introduce a deep notch (single castellation) for relaxing the stress in the embrittled armour [23]
- or to replace the W blocks with Cr blocks brazed to flat W tiles as armour for taking the benefits of extremely low activation behavior and the lower ductile-to-brittle transition temperature of chromium.

3.2.2. Exhaust power distribution overview A first assessment of divertor limitations in DEMO has been reported in [44]. To provide an overview of the power exhaust situation, we summarize a set of 0D parameters related to power exhaust in table 3. The column *Ref* displays the situation for `EU DEMO1 2015` assuming a fraction of

Table 3. A set of 0D parameters related to power in `EU DEMO1 2015`

Parameter	Unit	Ref	$f_{rad,core} \downarrow$	$f_{rad,SOL} \downarrow$	$S \downarrow$
R	m	9.1	9.1	9.1	9.1
P_{α}	MW	407.4	407.4	407.4	407.4
P_{aux}	MW	50	50	50	50
P_{LH}	MW	132	132	132	132
P_{sep}	MW	154	215	154	154
$f_{rad,core}$	1	0.66	0.53	0.66	0.66
$f_{rad,SOL}$	1	0.24	0.24	0.19	0.24
$f_{rad,tot}$	1	0.90	0.77	0.85	0.90
$P_{tar,tot}$	MW	46	106	67	46
$P_{tar,out}/P_{tar,tot}$	1	0.67	0.67	0.67	0.67
λ_q	mm	1.0	1.0	1.0	1.0
S	mm	4.4	4.4	4.4	1.5
λ_{int}	mm	8.2	8.2	8.2	3.5
$B_{pol,m}/B_{phi,m}$	1	0.3	0.3	0.3	0.3
$\theta_{\perp}$	deg	3	3	3	3
α	deg	1	1	1	1
$A_{wet,out}$	m^2	2.0	2.0	2.0	0.8
$q_{max,out}$	MW/m^2	15	35	22	36

radiation outside the separatrix of $f_{rad,SOL} = 0.24$ corresponding to a total radiation fraction $f_{rad,tot} = 0.90$. A midplane power decay length $\lambda_q = 1mm$ [44] and a divertor broadening $S = 4.4mm$ are assumed. The latter is based on [45] in combination with the assumption that S can be interpreted as the perpendicular diffusion in the divertor and hence scales with the connection lengths. Using equation (4) of [44] in combination with $\theta_{\perp} = 3°$ and $\alpha = 1°$ [44] leads to a peak power flux density of $15MW/m^2$.
It has to be noted, that the description of the divertor power flux profile in terms of λ_q and S is developed for attached plasmas and the plasma in DEMO is planned to be detached. The table also shows variations of the case *Ref.* It can be seen that a reduction of the radiation fraction inside respectively outside the separatrix by 20% leads to an increase in the peak power flux density to $35MW/m^2$ respectively $22MW/m^2$. Replacing the divertor broadening by a less optimistic value of $1.5mm$ leads to an increase of the peak power flux density to $36MW/m^2$.

3.2.3. Initial SOLPS calculations A more detailed investigation of the possibility of divertor protection in DEMO has been carried out employing the code SOLPS-5.1 [46]. Figure 4 shows the domain extending from the pedestal region to the SOL, which is represented by a mesh of 96 poloidal and 36 radial cells. In these initial investigations a relatively large number of data points have been produced, which differ in the electron density at the outer mid-plane, the combination of impurity species (N, Ar, Kr)‡ and their concentrations and the power crossing the inner domain boundary. To be efficient a reduced version of SOLPS with charge state bundling [47], no drift representation and a fluid neutral model has been used. A fixed impurity concentration at the core boundary has been assumed. In future simulations this setup is planned to be replaced by impurity sources in realistic positions, which would allow for more realistic ratios of the impurity concentration in core and divertor.

‡ He and W impurities have not been accounted for.

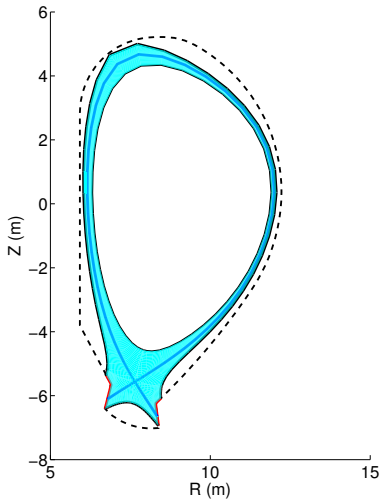

Figure 4. Domain of the SOLPS calculations colored in light blue. Also shown are the separatrix and the first wall contour (dashed).

The idea of the investigation was to identify simulations fulfilling the criteria (1) $P_{sep} \geq 150MW$, (2) $T_{e,max,tar} \leq 4eV$ and (3) $q_{max,tar} \leq 10MW/m^2$. In the set of simulations that has been performed until now these criteria where almost met using the impurities Ar and Xe. Table 4 list several parameters of the SOLPS simulation for DEMO, that is most in line with the criteria. The impurity concentrations at the core boundary are very close to the concentrations in a study with a much rougher representation of the SOL and divertor and a more detailed representation of H-mode access and fulfilling the burn condition (subsection 6.1. in [4]). Transport coefficients corresponding to a mid-plane e-folding length $\lambda_q \approx 1.5mm$ have been chosen. The power crossing the separatrix $P_{sep} = 175MW$ is 13% above the nominal value in `EU DEMO1 2015`.

The electron density at the separatrix mid-plane $n_{e,mp}$ corresponds to 68% of the Greenwald density. As it is not clear, if this is possible, the consistency of core and edge simulations for DEMO is questionable. To resolve this, a better understanding of the pedestal particle transport is urgently required. The fraction of radiation outside the separatrix $f_{rad,SOL} = 0.30$ is higher than in the 0D parameter set (table 3). The degree of detachment (DoD) expressed as the ratio of the separatrix pressure in the mid-plane and at the target has a value of 1.5. This corresponds to a relatively modest pressure loss § and suggests that there are further possibilities to reduce the peak power flux densities at the divertor.

The results described above have to be treated with care. Especially the fact that drifts are not represented and neutrals are modeled as a fluid are important in this context. We assume that the situation at the outboard midplane is modeled relatively reasonably. The relatively low power flux density at the inner target is very likely too low. The situation at the outer target needs to be confirmed in simulations with a kinetic neutral model.

§ A total pressure loss corresponds to DoD→ inf.

Table 4. Parameters of the SOLPS simulation for DEMO, that is most in line with the target criteria described in the text

Parameter	Unit	Value
$c_{ped,Ar}$	1	8.6×10^{-3}
$c_{ped,Kr}$	1	1.3×10^{-4}
$c_{SOL,Ar}$	1	1.1×10^{-2}
$c_{SOL,Kr}$	1	1.4×10^{-3}
λ_q	mm	$\approx 1.5mm$
P_{sep}	MW	175
$n_{e,mp}$	$10^{19}m^{-3}$	5.0
n_{GW}	$10^{19}m^{-3}$	7.3
$f_{rad,SOL}$	1	0.30
$P_{tar,out}$	MW	28
$P_{tar,in}$	MW	8
$T_{e,max,out}$	eV	3.3
$T_{e,max,in}$	eV	0.7
$q_{max,out}$	MW/m^2	17
$q_{max,in}$	MW/m^2	3

3.3. First Wall Loads

Compared to ITER, in `EU DEMO1 2015` a roughly 4 times higher fusion power has to be distributed to a wall area that is about 1.7 times larger. Additionally the peak power flux density that can be deposited to the standard wall component (highest energy conversion and breeding efficiency) is assumed to be about $1MW/m^2$ [3], which is compares to the highest power handling capability of the first wall in ITER outside the divertor of $4.7MW/m^2$. Hence the design of a first wall for DEMO, which is in line with all constraints, was identified as a severe challenge that has to be addressed from the very early design phase. In this subsection a brief overview of the state of the investigations to estimate wall loads in DEMO is provided. The focus is on the most important non-disruptive load cases and discuss wall loads during disruptions in subsection 3.4.

A first review of wall loads in DEMO focusing mainly on steady state loads is provided in [3]. The main static heat load contributions are due to thermal charged particles and radiation. To estimate thermal charged particle loads, following quantities associated with high uncertainties have to be estimated: (1) the maximum steady state power crossing the separatrix, (2) fraction of this power that goes into the blobby transport and (3) the associated radial e-folding length. While the first quantity needs to be determined by control investigations, (2) and (3) are important DEMO physics gaps (section 2). After initial wall design optimization, 3D calculations [48] arrive at thermal charged particle loads, which are highest at the top of the machine with values up to $0.7MW/m^2$ (plasma assumptions: $P_{sep,max} = 1.5 \times P_{sep,nom} = 231MW$, of which 30% is distributed with $\lambda_q = 50mm$). The investigation of the effects of deviations of the machine and plasma from the idealized assumptions in these calculations will lead to higher potential peak values. To reduce these, an increase of the wall clearance might be necessary.

Radiation facilitated by impurity seeding is the preferred power exhaust channel for DEMO. However due to the expected high level of x-point radiation, especially in the

outboard baffle (distance to x-point $\approx 1m$) significant loads are expected. Assuming a fraction of x-point radiation of 1/3 leads to a peak power flux density of $0.50MW/m^2$ and to a total power flux density of $0.77MW/m^2$ in this area [3]. The power flux density in the outer baffle region due to x-point radiation scales roughly with the inverse of the distance to the x-point. Hence, there is limited possibility to reduce this value by design, if necessary.
An initial 0D investigation of the steady state wall erosion in DEMO by charge exchange neutrals and impurity ions has been carried out [49]. A broad range of plasma background situations has been considered. The conclusion is that erosion of the wall does not pose a constraining limitation, if two assumptions are made: (1) The plasma wall clearance is 22.5cm (minimum value in `EU DEMO1 2015`) or larger. (2) It is acceptable to erode 50% of the W layer thickness on the first wall. It is essential to confirm this initial result by further studies - ideally with poloidal resolution.
The limited configuration (i.e. separatrix defined by first wall contact location) in the ramp-up and ramp-down are associated with extreme local heat loads at the first wall. An initial discussion of assumptions to estimate the heat load evolution during these phases has been presented in [3]. First investigations of designs with 18 limiters ‖ in the midplane ports and $P_{sep} = 5MW$ find peak power flux densities at the limiters of about $1MW/m^2$. For the limiter design a number of technologies can be used, which have power handling capability up to divertor W mono-block technology.
In addition to the relatively low steady state power handling capability of the standard wall component in DEMO defined by the temperature limit of EUROFER-97, also significantly concern is related to the W surface melt limit. Hence, dynamic power loads and their effects need to be anticipated to steer the design in an appropriate way, if possible. To study non-disruptive events in DEMO leading to temporary enhanced heat loads, currently a representative set of plasma disturbances is developed, for which the evolution of equilibrium and wall heat loads will be evaluated. Initial results for the cases *minor disruption* (recovered, $\Delta\beta_{pol} = -0.1$, $\Delta li = -0.1$) and *ELM* ($\Delta\beta_{pol} = -0.1$, $\Delta li = +0.1$) show loads that can be handled without or by modest design modifications. Also related - four different scenarios for unforeseen H-L-transitions are under and development and will be investigated in a similar way.
In summary, to keep first wall loads in DEMO within the technical limits poses a significant challenge - especially when compared to ITER. However, there is indication that the non-disruptive part of this problem can be managed by appropriate design of the plasma and the device. These measures include the increase of the plasma-wall-clearance and the integration of limiters and other components with advanced load handling capability, which imply a reduction of the fusion power, energy conversion or breeding efficiency.

3.4. Disruptions

Disruptions in DEMO are associated with an outstanding potential risk in terms of machine protection or even safety. `EU DEMO1 2015` has a thermal stored energy of 3.7 times and a plasma current of 1.3 times the ITER value. Due to this disruptions need to be addressed from a very early design phase. The preliminary DEMO disruption investigation strategy has two main program components:

- Determine acceptable disruption rates for a representative set of worst case

‖ Not compatible with other systems that should be allocated in these ports!

disruptions with/without mitigation: This includes the prediction of the evolution of these events and the associated loads and the comparison to the limits of optimised components.

- Identify ways to achieve the required disruption rates: This includes the choice of the operating point in system code studies, system hardware redundancy optimisation, the specification of mitigation systems and the development of disruption related plasma control schemas.

The prediction of the evolution of worst case disruptions with/without mitigation concentrates in the first phase on the thermal quench making following general assumptions:

- Nominal thermal energy content during flat-top: 1.3GJ
- Pre disruption power e-folding length: 1mm [44]
- Broadening factor of power e-folding length: 7 [50] ¶
- Thermal quench duration: Rise phase: 1ms, decay phase 3ms [3]

Two types of unmitigated disruptions have been simulated: Upward vertical displacement event (VDE) and centered disruption (CD). In a first step the evolution of the equilibrium is predicted using CarMa0NL [51] accounting for the Grad-Shafranov equation and the electromagnetic interaction between plasma and 3D conducting structures including halo currents. After this the temporal evolution of wall loads by charged thermal particles is calculated in 2D [8]. The anticipated underestimation due to the idealized plasma and wall geometry is compensated by multiplying all charged particle heat loads by a factor of 10 (first wall) respectively 2 (divertor). Radiation loads during mitigated disruptions have been calculated by a Monte-Carlo approach similar to the one used for the evaluation of static loads reported in [4]. It has to be noted that the presented calculations do not account for vapor shielding, which has the potential to significantly reduce the peak heat impact factor at the component especially in case of fast events [52].
In the VDE simulation the plasma moves vertically and goes into limiter configuration. 145ms later $q_a = 2$, which assumed to be the starting condition for the thermal quench. It is assumed, that at this time $W_{th} = 0.5W_{th,nom} = 0.65GJ$ [53]. Figure 5(a) shows the wall energy density during the thermal quench. The peak energy density during this 4ms is $165MJ/m^2$ corresponding to heat impact factors of $2609MJ/(m^2\sqrt{s})$, which is far above the W surface melt limit [54].
A CD has been simulated assuming $W_{th} = 0.65GJ$ at the onset of the thermal quench. Figure 5(b) shows the wall energy density during the thermal quench. In this case the energy densities are moderate at the first wall but extreme at the divertor reaching values up to $160MJ/m^2$ corresponding to a heat impact factor of $2530MJ/(m^2\sqrt{s})$.
For the simulation of a mitigated disruption in DEMO following assumptions are made: (1) 20% of the nominal thermal energy is radiated in the pre-thermal-quench phase in 8ms, (2) 64% of the nominal thermal energy is radiated in the thermal quench phase in 1ms, (3) 16% of the nominal thermal energy is conducted/convected in the thermal quench phase in 1ms, (4) Toroidal radiation peaking factor: 2 (5) Poloidal radiation peaking factor: 1.4.
Figure 6 shows the components of the wall load for the CD. In the thermal quench the radiation load peaks at $1MJ/m^2$. The Corresponding heat impact factor of

¶ Starting from thermal quench onset

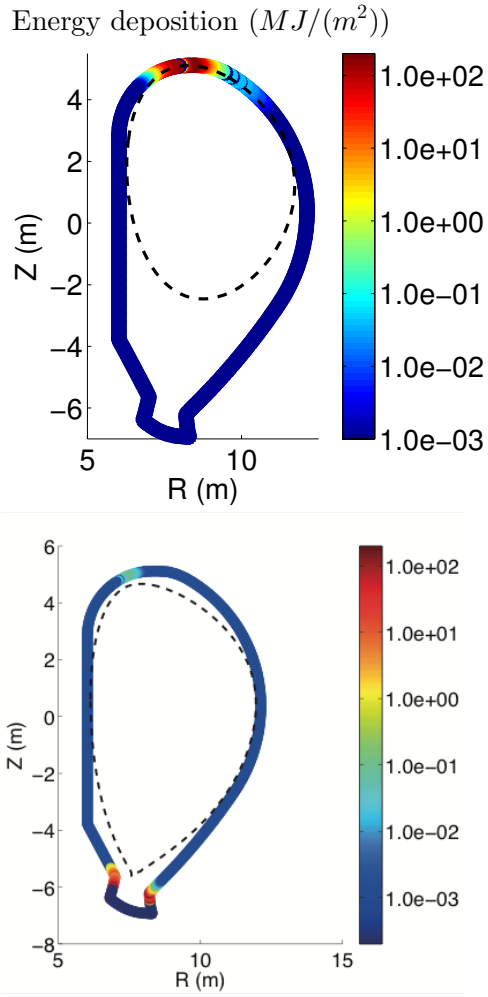

Figure 5. (a) Energy density during the thermal quench of a vertical displacement event: It is assumed that $W_{th} = 0.5W_{th,nom} = 0.65GJ$ at the thermal quench onset. The dashed lines represent the separatrix position. (b) Energy density during the thermal quench of a central disruption: It is assumed that $W_{th} = 0.5W_{th,nom} = 0.65GJ$ at the thermal quench onset. The dashed lines represent the separatrix position.

$32MJ/(m^2\sqrt{s})$ is significantly above the W crack limit. The load conducted/convected by charged particles has a peak in the divertor of $17MJ/m^2$ (heat impact factor $531MJ/(m^2\sqrt{s})$).

In addition to these studies of fast transients during disruptions also other phases need to be investigated. Especially during the current quench phase of an unmitigated disruption, which is predicted to have a minimum duration of $\approx 70ms$, a big fraction of the poloidal magnetic energy of 1.3GJ is converted into thermal loss power. In such a slower event the mitigating effect of vapor shielding will be clearly reduced and there is the risk of boiling the coolant and a subsequent catastrophic cooling pipe burn out.

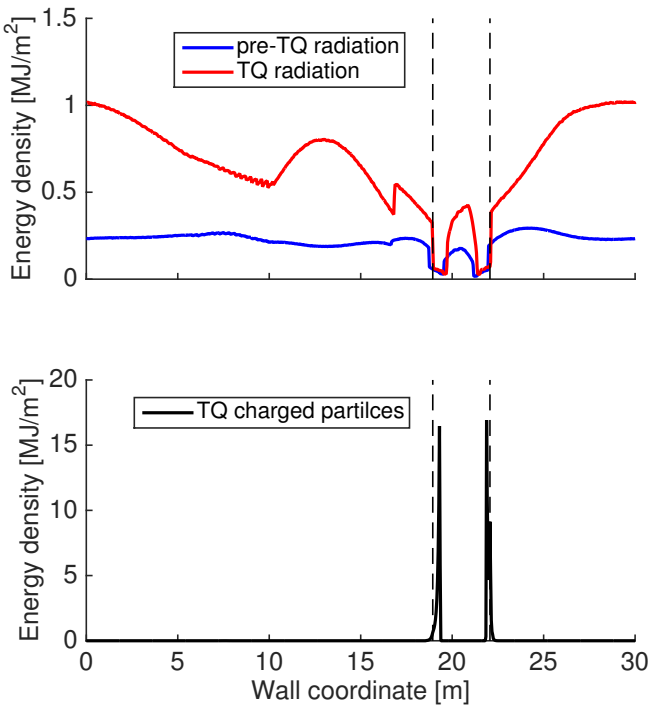

Figure 6. Simulation of a mitigated disruption: (a) Radiation energy density during pre-thermal-quench and thermal quench as a function of the wall coordinate. (b) Convected/conducted energy density during thermal quench as a function of the wall coordinate. The dashed vertical lines mark the transition between divertor and breeding area.

Also, next to loads from thermal charged particles and radiation, the effect of runaway electrons generated in the current quench phase has to be investigated. Their effect on the first wall components needs to be understood for the DEMO case (all W PFC).

The final objective of these studies is to understand the destructive effect of several types of disruptions including the most severe ones for the options *mitigated* and *unmitigated*. Based on this information the DEMO design (e.g. first wall limiters) can be optimized to reduce the level of destructivity. In the following, for a given design rate limits for the events need to be defined, which are compatible with fulfilling the mission of DEMO. In principle minimization and prediction of the rate of the set of events would be necessary. We distinguish between (1) disruptions caused by component failures and (2) other - mainly plasma scenario driven disruptions. In both areas a significant increase of knowledge is required.

4. Summary

Section 2 of this publication provides a systematic overview of DEMO Physics Gaps structured in feasibility gas and performance gaps. It becomes evident that in the

next decades a significant expansion and consolidation of the physics knowledge for DEMO has to happen. This has to be accomplished via experiments in various devices including ITER, simulations and theoretical studies. An overall strategy, that describes for each gaps activities to partly or fully close it, is under development.

The bulk of the publication summarizes recent progress in the development of the DEMO Physics Basis in four areas of central importance. Application of the recently developed x-point displacement criterion suggest that ELM mitigation in DEMO using ex-vessel coils is possible with currents of 200kAt. This criterion describes in a relatively uniform way mitigation results from various experiments. However it is not clear, if in DEMO ELM mitigation is sufficient in terms of divertor protection, or, if complete ELM suppression would be required. Another investigation in this context applies a recent scaling of the ELM energy density to DEMO. If the ELM mitigation scenario for DEMO follows this scaling, severe reductions of the pedestal density and temperature would follow, unless a solution is found that significantly reduces the relative ELM size and keeps the pedestal top density and temperature largely unchanged.
The steady state protection of the DEMO divertor has been identified to be a challenge. Section 3.2.1 provides an overview of the status of the divertor technology development starting from the ITER-like W mono-block concept. New design concepts tailored to better cope with the more challenging loading conditions in DEMO are being developed and a subset of them has withstood the ITER heat flux loads (300 load cycles at $20MW/m^2$). An overview of the 0D power exhaust parameters consistent with `EU DEMO1 2015` provides some insight in the relevance of several key uncertainties. Also initial calculations with a relatively reduced version of SOLPS are presented. The parameters in this simulation are largely consistent with the 0D power exhaust parameters. On the one side there seems to be scope for optimization of the adjustable parameters (e.g. impurity concentrations, power crossing the separatrix). On the other side it is very important to consolidate the runs by simulations with more complete physics models. Important uncertainties are related to the transport coefficients and the density at the separatrix.
Also the loads at the first wall exhibit a significant challenge for the design of DEMO. The most important mechanisms are conduction/convection of charged thermal particles and radiation. There is some indication that the steady state loads and loads due to non-disruptive perturbations can be managed by appropriate design of the plasma and the device. However, these solutions can reduce the gross electric power or the T breeding rate.
Protecting DEMO against destructive disruption effects is potentially the most significant challenge of the DEMO concept design development. Charged particle and radiation loads during unmitigated disruptions lead to heat impact factors, which are clearly above the melt threshold at the first wall. Also mitigated disruptions are lead to significant heat loads at the wall and even more at the divertor. Several effects (e.g. runaway electrons) need to be investigated in the future. It is clear, that DEMO needs to have a very high number of full power discharges with an extremely low rate of disruptions. This points in a direction that the DEMO design has to be much more robust against disruptions than any tokamak design before and that the rate of disruptions must be much lower than in present devices and ITER.

Acknowledgment

This work has been carried out within the framework of the EUROfusion Consortium and has received funding from the Euratom research and training programme 2014-2018 under grant agreement No 633053. The views and opinions expressed herein do not necessarily reflect those of the European Commission.
The work is partly funded by National National Magnetic Confinement Fusion Science Program under grant No. 2014GB107004 and National Natural Science Foundation of China (NSFC) 11275041.

5. References

[1] Romanelli F *et al* *Fusion Electricity - A roadmap to the realisation of fusion energy* ISBN 978-3-00-040720-8, 2012
[2] Wenninger R *et al* 2017 *Nuclear Fusion* **57** 016011
[3] Wenninger R *et al* 2017 *Nuclear Fusion* **57** 046002
[4] Wenninger R *et al* 2015 *Nuclear Fusion* **55** 063003
[5] Federici G *et al* 2014 *Fusion Engineering and Design* **89** 882 – 889
[6] Wenninger R *et al* 2015 *42nd EPS Conf. on Contr. Fusion and Plasma Phys., Lisbon, Portugal*
[7] Turnyanskiy M *et al* 2015 *Fusion Engineering and Design* **9697** 361 – 364
[8] Wenninger R *et al* 2017 *to be sumitted to Nuclear Fusion*
[9] Puetterich T *et al* 2015 *42nd EPS Conf. on Contr. Fusion and Plasma Phys.*
[10] ITER Physics Expert Group on Energetic Particles, Heating and Current Drive and ITER Physics Basis Editors 1999 *Nuclear Fusion* **39** 2471
[11] Snyder P *et al* 2009 *Nuclear Fusion* **49** 085035
[12] Martin Y R, Takizuka T, and the ITPA CDBM H-mode Threshold Database Working Group 2008 *Journal of Physics: Conference Series* **123** 012033
[13] Carralero D *et al* 2017 *Nuclear Fusion* **57** 056044
[14] Zohm H 1996 *Plasma Physics and Controlled Fusion* **38** 105–128
[15] Burrell K H *et al* 2002 *Plasma Physics and Controlled Fusion* **44** A253
[16] Doyle E J *et al* 1991 *Physics of Fluids B: Plasma Physics* **3** 2300–2307
[17] Whyte D *et al* 2010 *Nuclear Fusion* **50** 105005
[18] Evans T E *et al* 2004 *Phys. Rev. Lett.* **92** 235003
[19] Evans T *et al* 2008 *Nuclear Fusion* **48** 024002
[20] Liu Y Q, Bondeson A, Fransson C M, Lennartson B, and Breitholtz C 2000 *Physics of Plasmas* **7** 3681–3690
[21] Ryan D A *et al* 2015 *Plasma Physics and Controlled Fusion* **57** 095008
[22] Paz-Soldan C *et al* Mar 2015 *Phys. Rev. Lett.* **114** 105001
[23] Li M and You J H 2016 *Fusion Engineering and Design* **113** 162 – 170
[24] Liu Y *et al* 2016 *Nuclear Fusion* **56** 056015
[25] Sun Y *et al* Sep 2016 *Phys. Rev. Lett.* **117** 115001
[26] Liu Y *et al* 2017 *Physics of Plasmas* **24** 056111
[27] Yang X *et al* 2016 *Plasma Physics and Controlled Fusion* **58** 114006
[28] Kirk A *et al* 2013 *Plasma Physics and Controlled Fusion* **55** 015006
[29] Kirk A *et al* 2015 *Nuclear Fusion* **55** 043011
[30] Eich T *et al* 2016 *PSI conference, Rome, Italy*
[31] Wenninger R *et al* 2016 *Power Handling and Plasma Protection Aspects that affect the Design of the DEMO Divertor and First Wall, FIP/P7-14, presented at 26th IAEA Int. Conf. on Fusion Energy, Kyoto*
[32] You J *et al* 2016 *Fusion Engineering and Design* **109111, Part B** 1598 – 1603 Proceedings of the 12th International Symposium on Fusion Nuclear Technology-12 (ISFNT-12)
[33] Raffray A *et al* 2010 *Fusion Engineering and Design* **85** 93 – 108
[34] You J *et al* 2016 *Nuclear Materials and Energy* **9** 171 – 176
[35] You J H 2015 *Nuclear Fusion* **55** 113026
[36] Merola M *et al* 2015 *Fusion Engineering and Design* **9697** 34 – 41 Proceedings of the 28th Symposium On Fusion Technology (SOFT-28)
[37] Pintsuk G *et al* 2015 *Fusion Engineering and Design* **9899** 1384 – 1388 Proceedings of the 28th Symposium On Fusion Technology (SOFT-28)
[38] Fabritsievand S A and Pokrovsky A S 1997 *Plasma Devices and Operations* **5** 133–141

[39] You J H 2015 *Nuclear Materials and Energy* **5** 7 – 18
[40] Maio P D, Garitta S, You J, Mazzone G, and Vallone E 2017 *Fusion Engineering and Design* –
[41] You J *et al* 2017 *Fusion Engineering and Design* –
[42] Li M, Werner E, and You J H 2015 *Fusion Engineering and Design* **90** 88 – 96
[43] Li M, Werner E, and You J H 2014 *Fusion Engineering and Design* **89** 2716 – 2725
[44] Wenninger R *et al* 2014 *Nuclear Fusion* **54** 114003
[45] Sieglin B *et al* 2016 *Plasma Physics and Controlled Fusion* **58** 055015
[46] Schneider R *et al* 2006 *Contributions to Plasma Physics* **46** 3–191
[47] Coster D P 2016 *Contributions to Plasma Physics* **56** 790795
[48] Firdaouss M, Riccardo V, Martin V, Arnoux G, and Reux C 2013 *Journal of Nuclear Materials* **438, Supplement** S536 – S539 Proceedings of the 20th International Conference on Plasma-Surface Interactions in Controlled Fusion Devices
[49] Beckers M, Biel W, Tokar M, and Samm U 2017 *Nuclear Materials and Energy* –
[50] Loarte A *et al* 2004 *IT/P3-34, presented at 26th IAEA Int. Conf. on Fusion Energy, Vilamoura, Portugal*
[51] Villone F, Barbato L, Mastrostefano S, and Ventre S 2013 *Plasma Physics and Controlled Fusion* **55** 095008
[52] Pestchanyi S, Pitts R, and Lehnen M 2016 *Fusion Engineering and Design* **109111, Part A** 141 – 145 Proceedings of the 12th International Symposium on Fusion Nuclear Technology-12 (ISFNT-12)
[53] Riccardo V, Loarte A, and the JET EFDA Contributors 2005 *Nuclear Fusion* **45** 1427
[54] Linke J *et al* 2008 *Proc. Forum 2008 of the World Academy of Ceramics, Chianciano Terme, Italy*